SCIENTIFIC REPORTS

OPEN

SUBJECT AREAS:
CLIMATE CHANGE
ATMOSPHERIC SCIENCE
HYDROLOGY
ENERGY

Thermal Controls on the Asian Summer Monsoon

Guoxiong Wu[1], Yimin Liu[1], Bian He[1,2], Qing Bao[1], Anmin Duan[1] & Fei-Fei Jin[3]

[1]State Key Laboratory of Numerical Modeling for Atmospheric Sciences and Geophysical Fluid Dynamics, Institute of Atmospheric Physics, Chinese Academy of Sciences, [2]Nanjing University of Information Science & Technology, [3]Department of Meteorology, University of Hawaii, Honolulu, Hawaii, USA.

Received
26 January 2012

Accepted
1 May 2012

Published
11 May 2012

Correspondence and requests for materials should be addressed to Y.L. (lym@lasg.iap.ac.cn)

The Asian summer monsoon affects more than sixty percent of the world's population; understanding its controlling factors is becoming increasingly important due to the expanding human influence on the environment and climate and the need to adapt to global climate change. Various mechanisms have been suggested; however, an overarching paradigm delineating the dominant factors for its generation and strength remains debated. Here we use observation data and numerical experiments to demonstrates that the Asian summer monsoon systems are controlled mainly by thermal forcing whereas large-scale orographically mechanical forcing is not essential: the South Asian monsoon south of 20°N by land–sea thermal contrast, its northern part by the thermal forcing of the Iranian Plateau, and the East Asian monsoon and the eastern part of the South Asian monsoon by the thermal forcing of the Tibetan Plateau.

The monsoon is generally considered an atmospheric response to seasonal changes in land–sea thermal contrast, induced by the annual cycle of the solar zenith angle[1,2]. The Asian summer monsoon (ASM) is the strongest element of the global monsoon system[3–5]. In addition to land–sea contrast, it is affected by large-scale mountain-ranges such as the Tibetan Plateau (TP)[6–9], which serve, in winter, as a giant wall across almost the whole Eurasian continent that blocks cold outbreaks from the north and confines the winter monsoon to the eastern and southern Asia[10]. The air over the TP descends in winter and ascends in summer, driving the surrounding surface air that diverges from the TP in winter and converges toward it in summer, much like a sensible-heat-driven air-pump (SHAP)[11,12]. Because in summer the impinging flow toward the TP is weak, TP-SHAP has been suggested to be dominant over mechanical forcing in controlling the ASM[9,12–14], including its subsystems: the South Asian summer monsoon (SASM) and the East Asian summer monsoon (EASM).

Variations in the ASM and its controlling factors are known to be influenced by natural fluctuations[15–17] along with anthropogenic greenhouse–gas emissions and environmental pollution[18,19]. The TP surface sensible heat flux has weakened in recent decades, due mainly to global warming[20,21]. The interception of solar radiation by atmospheric brown clouds leads to surface dimming[19]. In summer, the greater dimming over land than over adjacent oceans suggests a weakening in land–sea contrast; the dimming trend over the northern Indian Ocean leads to a decrease in local evaporation and less moisture being fed to the monsoonal inflow[22], as well as a decrease in the meridional sea-surface-temperature gradient[22,23]. These factors may contribute to the weakening of monsoonal rainfall[19]. In addition, the darkening of snow and ice due to the deposition of soot reduces surface albedo and enhances solar absorption[24,25], and heating of the troposphere over the TP due to increasing amounts of dust and black carbon aerosols can lead to enhanced land–atmosphere warming, which in turn accelerates snow melt and glacier retreat[26,27].

Global warming and widespread glacier-mass loss and snow-cover reduction are projected to accelerate throughout the 21st century[28]. These changes are expected to have a strong influence on certain regions of the ASM in which TP thermal forcing plays an important role. Many studies have examined the separate influences of individual factors on the ASM[3,6–9,11,12]; however, their relative and synthetic contributions to the ASM remain unclear, also it remains debated whether the "Himalayas wall" can block dry air from the north and contribute to the formation of the SASM[29]. In addition the impacts of another Plateau, the Iranian Plateau (IP), lower than the TP but with the same size, has never been paid attention. With the aim of resolving these issues, in the present study we performed numerical experiments to investigate the various factors that control different aspects of the ASM.

Results

Influence of land–sea thermal contrast on the ASM. The influence of land–sea thermal contrast and plateau forcing on the ASM is investigated by employing a general circulation model (GCM), FGOALS/SAMIL

(Methods). The model is integrated with prescribed, seasonally varying sea surface temperature (SST) and sea ice. The controlled climate integration is referred to as the **CON** experiment. The modelled precipitation (Fig. 1a) shows some bias compared with observations[30,31] (Fig. 1b), with a stronger Somali jet and enhanced rainfall over most of the ASM domain, but it captures the main features of the ASM, performing reasonably well in simulating the maximum centers over the western coast of India, the Bay of Bengal (BOB), and the southeastern slopes of the TP.

Since the monsoon is traditionally considered an atmospheric response to the seasonal land–sea thermal contrast[1,2], it is reasonable to infer that the precipitation forced not by orography but by the land–sea distribution alone could be considered as a monsoon prototype. A no-mountain experiment **NMT** is thus designed, being the same as the **CON** run except that all the mountains worldwide are removed (Methods Table 1). The modelled precipitation (Fig. 1c) is confined to south of 20°N, with the maximum centers (>18 mm·d^{-1}) located between 10°N and 15°N, as in the control run. Remarkable changes compared with the control run are seen in the subtropical area: the SASM north of 20°N and the EASM are substantially reduced. Because our main concern is how the extensive Asian mountains of the IP and TP (IPTP) influence the ASM, in the next experiment only the IPTP is removed. The simulated precipitation pattern (Fig. 1d) is similar to that in **NMT** (Fig. 1c) and is considered the component of the ASM that is induced by land–sea thermal contrast alone. The experiment is thus termed the **L_S** experiment (See Methods Experiment Design).

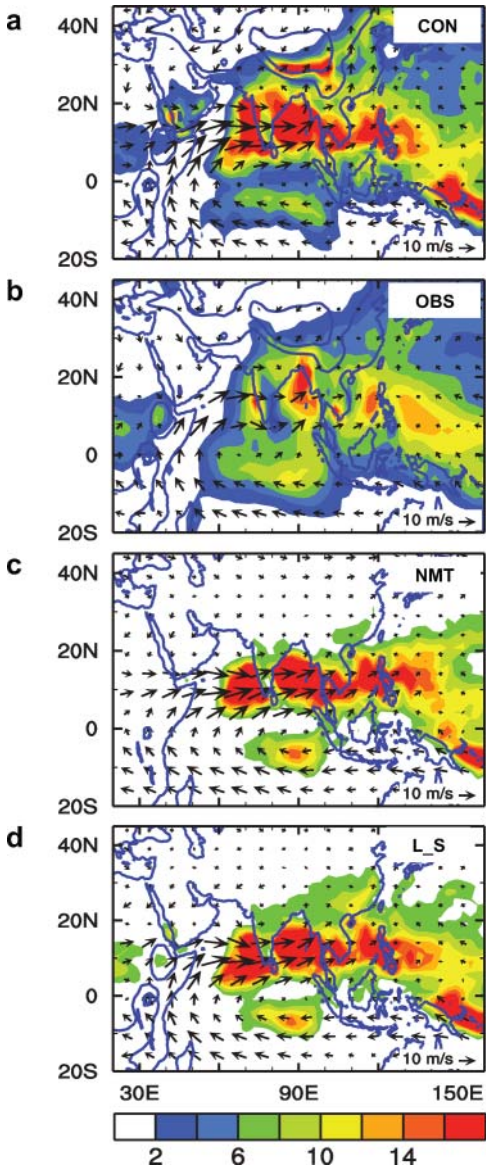

Figure 1 | Impacts of land–sea thermal contrast on the Asian summer monsoon, showing the summer precipitation rate (color shading, unit mm·d^{-1}) and 850 hPa winds (vectors) for a, the control experiment CON; b, observations averaged over the period 1979–2009 from Global Precipitation Climatology Project (GPCP) for precipitation and from NCEP-DEO AMIP-II Reanalysis (R-2) for winds; c, experiment NMT in which the global surface elevations are set to zero; and d, experiment L_S in which only the elevations of the Iranian Plateau (IP) and the Tibetan Plateau (TP) are set to zero. Thick contours indicate elevations higher than 1,500 m and 3,000 m.

Influence of IPTP mechanical insulation on the ASM. The differences (**DIFF**) in circulation and precipitation between **CON** (Fig. 1a) and **L_S** (Fig. 1d), as shown in Fig. 2a, are forced by mechanisms other than land–sea thermal forcing. Such mechanisms are required to (1) produce a cyclonic circulation at 850 hPa over the subtropical continent between 20°N and 40°N, circumambulating the IPTP; (2) reduce precipitation over tropical oceans and the northwestern Pacific; and (3) increase precipitation mainly over the Asian continent, with maximum centers over India, the northern BOB, the southern slopes of the TP, and eastern Asia.

The absence of precipitation over northern India in the **L_S** experiment might reflect the removal of the "IPTP insulator," which results in the southward advection of dry, cold air from the subtropics and a lack of tropical convective instability and rainfall. Were this the case, merely adding the IPTP (but not allowing its surface-sensible-heating to heat the atmosphere) into the **L_S** experiment, which is defined as the **IPTP_M** experiment (See Methods Experiment Design), would be sufficient to produce the monsoon rainfall in the northern South Asia. However, the results in Fig. 2b indicate that this is not the case. In the **IPTP_M** experiment, the patterns of both precipitation and circulation at 850 hPa are similar to those in the **L_S** experiment. Similarly, if we merely add IP and TP separately into the **L_S** experiment (i.e., the **IP_M** and **TP_M** experiments, respectively), the resultant precipitation and circulation distributions (Fig. 2c and 2d, respectively) are also similar to those in the **L_S** experiment. These results demonstrate that in summer, mechanical insulation of the IP and TP has a minor influence on the generation of the ASM, as it cannot produce the required compensating rainfall and precipitation patterns (Fig. 2a).

Influence of IPTP thermal forcing on the ASM. Three sets of experiments were designed with surface sensible heating on the IP (**IP_SH**), TP (**TP_SH**), and IPTP (**IPTP_SH**) (Methods Experiment Design), in order to study the influence of orographically elevated thermal forcing on the ASM. In **IP_SH** (Fig. 3a), the IP thermal forcing generates a cyclonic circulation encircling the IP, similar to the western parts of the compensating circulation in Fig. 2a. The forcing also results in reduced precipitation, mainly over the tropical Indian Ocean and the northwest Pacific, and increased precipitation over the Asian continent west of 100°E (especially over Pakistan, northern India, and the southwestern slopes of the TP), a pattern similar to that of the compensating precipitation west of 100°E, indicating the important role of the IP in generating the northern SASM.

In the **TP_SH** experiment (Fig. 3b), TP thermal forcing also generates a cyclonic circulation encircling the TP. Correspondingly, reduced precipitation occurs west of 80°E; in contrast, increased precipitation occurs east of 80°E, especially over the BOB, the southern slopes of the TP, and East Asia. They are similar to the compensating precipitation and circulation patterns in the region east of 80°E (Fig. 2a), indicating that TP thermal forcing plays a dominant role in the generation of the EASM and the eastern part of the SASM.

Table 1 | Experiment design for examination of the dominant control of land-sea thermal contrast, as well as orographically mechanical insulation and elevated thermal impacts on the various parts of the Asian summer monsoon. The sign (√) indicates that the corresponding element has been included in the related experiment

Experiment Abbreviation	Land-sea thermal contrast	Orographically mechanical insulation		Orographically elevated thermal control	
		Iran Plateau (IP)	Tibet Plateau (TP)	Iran Plateau (IP)	Tibet Plateau (TP)
CON	√	√	√	√	√
NMT	√				
L_S	√				
IPTP_M	√	√	√		
IP_M	√	√			
TP_M	√		√		
IPTP_SH				√	√
IP_SH				√	
TP_SH					√
HIM	√	√	Southern slope only	√	√
HIM_M	√	√	Southern slope only		

In the **IPTP_SH** experiment (Fig. 3c), the elevated IPTP heating results in reduced precipitation in tropical oceans, and increased precipitation over the Asian continent to the north. The heating also generates a cyclonic circulation at 850 hPa over the Asian subtropical continental areas, with relatively isolated centers over the IP and TP. The results shown in Fig. 3c are basically equivalent to the linear addition of the results in Fig. 3a and 3b, indicating the important but contrasting roles of IP and TP thermal forcing in different parts of the ASM. More significantly, the precipitation and circulation patterns generated by IPTP thermal forcing (Fig. 3c) are close to those required to compensate the ASM (Fig. 2a). This result demonstrates that in addition to land–sea thermal contrast, the thermal forcing of large mountain ranges in Asia is an important factor in producing the ASM, especially over continental areas.

Influence of climbing versus deflecting orographic effects on the ASM. More than 85% of the total atmospheric water vapor, as measured by specific humidity, generally resides in a layer below 3 km above sea level. In order for monsoon clouds and precipitation to form, lower-tropospheric water vapor must be lifted by vertical motions forced either internally or externally; consequently, high near-surface moist entropy and warm upper-level temperature are coupled[32]. One of the internal forcing is the type of cold/warm fronts[33]. This mechanism is important at middle and high latitudes, especially in winter, but is not important in the tropics in summer because the air temperature in the tropics is relatively uniform.

The mechanical forcing of mountains is an important external forcing: air flow impinging upon mountains is either deflected to produce encircling flow or lifted to produce climbing flow[34,35]. Consequently, clouds and precipitation are generated around mountains. However, if a mountain is higher than several hundred meters, the conservation constraint of angular momentum and energy means that the airflow passes around the mountain rather than rising over it[36].

Thermal forcing can also generate atmospheric ascent, because large-scale atmospheric potential temperature (θ) increases with height. According to the steady-state thermodynamic equation

$$\vec{V}\cdot\nabla\theta = Q, \qquad (1)$$

where $\vec{V}$ is air velocity, in regions of heating ($Q>0$), air should penetrate isentropic surfaces upward. There are several types of atmospheric heating. Shortwave radiation is weakly absorbed directly by the atmosphere. In the absence of cloud, longwave radiation can easily escape into space. Condensation heating normally occurs above the cloud base. Whereas surface sensible heating can increase the near-surface entropy, result in the development of convective instability and trigger atmospheric ascent; and is effective in generating atmospheric ascent in the lower troposphere.

If surface sensible heating occurs on a mountain slope, and if the mountain is high enough, large amounts of moisture in lower layers are readily transported to the free atmosphere[12]. The TP in summer is a heat source for the atmosphere[6] and has a strong influence on weather and climate[9,11,12,37]. When a moist and warm southwesterly approaches the TP, the air becomes heated, starts to penetrate isentropic surfaces, and slides upward along its sloping surface.

Figure 4 shows the distribution of precipitation and streamlines at the $\sigma = 0.89$ surface, which is about 1 km from the surface. In the **CON** experiment (Fig. 4a), when the water conveyer belt originating from the Southern Hemisphere meanders eastward through the South Asian subcontinent, the effects of land–sea thermal forcing mean that severe precipitation centers are formed along 15°N. The rest of the water vapor is transported to sustain the East Asian Monsoon, although some swerves northward over northern India and the BOB. The pumping effect of TP-SHAP results in the convergence of air toward the TP. The upward streamlines are subperpendicular to the TP contours, eventually forming a cyclonic circulation at the southeastern corner of the TP. Consequently, heavy monsoon rainfall occurs over northern India and western China, with a maximum center (>18 mm·d^{-1}) appearing over the southeastern slopes of the TP. The condensation heating of this rainfall center generates cyclonic circulation in the lower layer and further intensifies the EASM, implying a positive feedback between precipitation and circulation[38].

In the IPTP_M experiment (Fig. 4b), in contrast, when the water vapor flux from the main water conveyer belt approaches the TP, it is not heated and the airflow remains at the same isentropic surface (Equation (1)). Consequently, the streamlines do not climb up the TP; instead, they move around the mountains, parallel to orographic contours. Thus, no monsoon develops over northern India and the TP, and the EASM is substantially weakened. These results indicate that the thermal forcing of large-scale mountains plays a dominant role in the generation of the northern and eastern parts of the SASM and the EASM.

A recent study based on numerical sensitivity experiments[29] emphasized the importance of the insulation effect of the

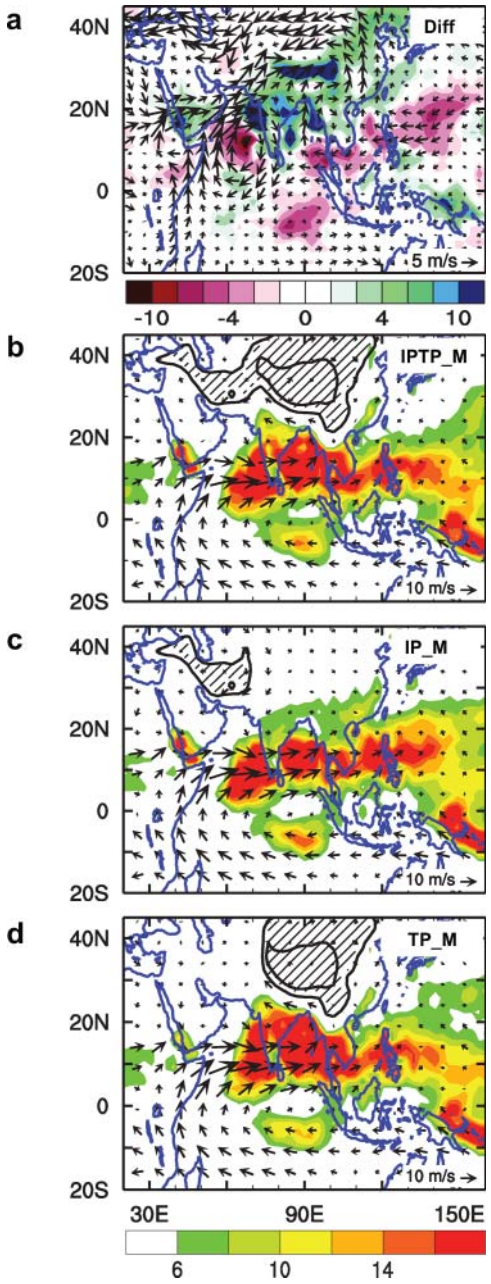

Figure 2 | Impacts of mountain mechanical forcing on the Asian summer monsoon, showing the summer precipitation rate (color shading, unit mm·d^{-1}) and 850 hPa winds (vectors) for a, the difference (DIFF) between the CON and L_S experiments, indicating the compensating rainfall and circulation required to make up the total monsoon; b, experiment IPTP_M in which the IP and TP mechanical forcing exists; c, experiment IP_M in which the IP mechanical forcing exists; and d, experiment TP_M in which the TP mechanical forcing exists. Thick black contours surrounding grey-hatched regions indicate elevations higher than 1,500 m and 3,000 m.

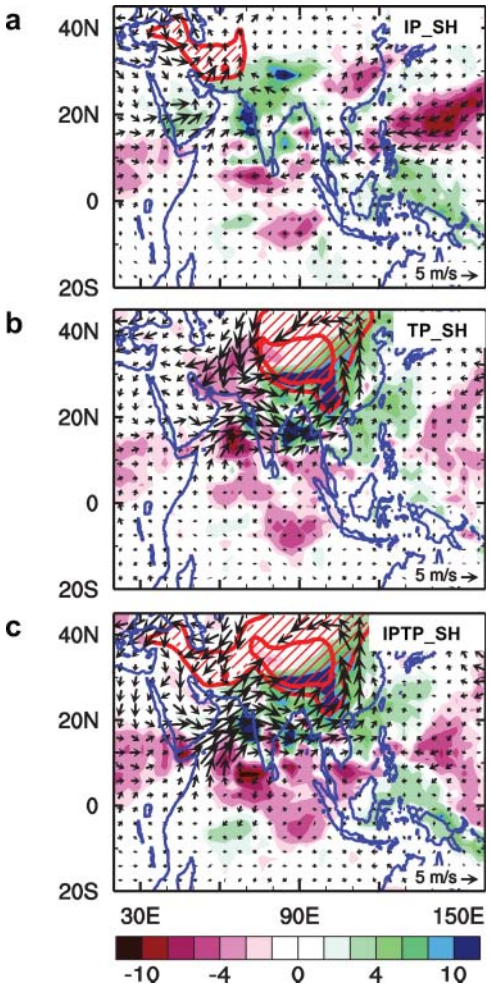

Figure 3 | Impacts of mountain thermal forcing on the Asian summer monsoon, showing the summer precipitation rate (color shading, unit mm·d^{-1}) and 850 hPa winds (vectors) generated due to the elevated surface sensible heating of a, the Iranian Plateau (IP_SH); b, the Tibetan Plateau (TP_SH); and c, the IP and TP (IPTP_SH). Thick red contours surrounding red-hatched regions indicate elevations higher than 1,500 m and 3,000 m.

Himalayas in producing the SASM. This finding is questionable because the experiment design took into account both the mechanical effect and surface sensible heating of the Himalayas and adjacent mountains (Fig. 4c); thus, the TP-SHAP mechanism still operates for the SASM. To demonstrate this point, we employed the current GCM and designed a sensitivity experiment (**HIM**) in which we followed Boos and Kuang's approach exactly in considering the effect of the Himalayas on the SASM (Methods Experiment Design), as indicated by the polygon in Fig. 4c. In addition to this tracking experiment, another experiment (**HIM_M**) was performed, which was the same as the **HIM** experiment except that the Himalayas' surface-sensible-heating was not allowed to heat the atmosphere (Fig. 4d). The results show that the **HIM** experiment (Fig. 4c) yields a similar SASM to that in the **CON** experiment (Fig. 4A), the same consequence as in Boos and Kuang. However, in the **HIM_M** case (Fig. 4d), the impinging tropical flow cannot climb up the TP; instead, it splits into eastern and western branches that each move around the TP, subparallel to orographic contours. The western branch forms a return flow, causing a southward shift in the Indian monsoon trough from its usual location over northeastern India to over central India. In this situation, the part of the SASM over northeastern India disappears, and the EASM is markedly weakened. These results demonstrate that the insulation effect of the TP is insignificant in terms of the ASM. Instead, it is the thermal forcing of the Tibetan/Iranian Plateau that plays a dominant role in the generation of the northern part of the SASM and the EASM.

Structure of the SASM. A striking feature of the present experiments is the insensitivity of the southern part of the SASM to IPTP forcing: in all experiments (Figs 1 and 2), the intensity and spatial distribution of precipitation south of 20°N show little change compared with the control while the configuration or thermal status of the Tibetan/Iranian Plateau shows a marked change. Figures 5a and 5b show 80°E–90°E longitudinally averaged

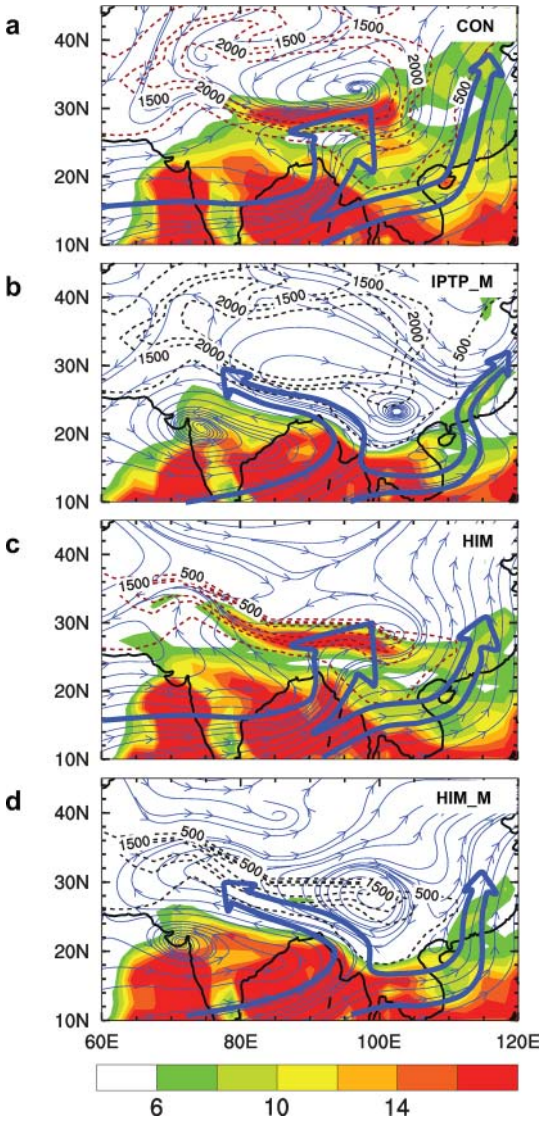

Figure 4 | Mechanism-- Relative contributions of the climbing and deflecting effects of mountains, showing the summer precipitation rate (color shading, unit mm·d^{-1}) and streamlines at the σ = 0.89 level for a, the CON experiment; b, the IPTP_M experiment; c, the HIM experiment; and d, the HIM_M experiment. Dashed contours surround elevations higher than 1,500 m and 3,000 m, with red and black colors respectively indicating with and without surface sensible heating of the mountains. Dark blue open arrows denote the main atmospheric flows impinging on the TP, either climbing up the plateau (**a** and **c**) or moving around the plateau, parallel to orographic contours (**b** and **d**).

latitude–height cross sections from the **CON** and **IPTP_M** experiments, demonstrating that the vertical velocity is divided into a southern branch and a northern branch at about 25°N. In the **CON** run (Fig. 5a), strong rising associated with the southern SASM is located over the northern Indian Ocean. Ascending air is also dominant above the TP, with maxima located near the surface, indicating the importance of surface sensible heating in generating orographic ascent. In the **IPTP_M** experiment (Fig. 5b), the lack of surface heating on the TP results in two remarkable sinking centers over its slopes; thus, the northern branch of the SASM disappears over northern India. However, the intensity and location of the southern branch is largely unchanged. In fact, in all the experiments the southern SASM branch remains steady, with a center (>18 × 10^{-2} Pa·s^{-1}) at about 400 hPa, locked to the south of the coastline. The insensitivity of the southern branch of the

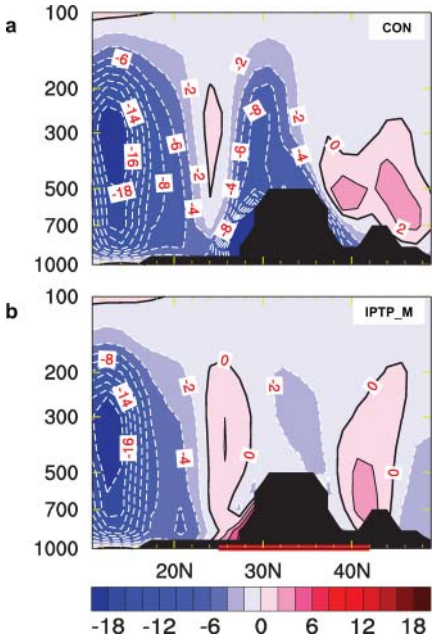

Figure 5 | Structure of the South Asian summer monsoon, showing 80°E–90°E longitudinally averaged vertical–meridional cross-sections of pressure vertical velocity (contour interval, 2 × 10^{-2} Pa·s^{-1}) for experiments a, CON; and b, IPTP_M.

SASM to orographic change indicates that the land–sea thermal contrast plays a dominant role in its generation and variation.

The above discussion is summarized schematically in Figure 6. The meridional circulation of the SASM can be divided into southern and northern branches. Its southern branch is located in the tropics: water vapor that originates from the Southern Hemisphere and is transported along the zonally oriented "water-vapor conveyer belt" is lifted upward due to the land–sea thermal contrast, forming monsoon precipitation there. The northern branch occurs along the southern margin of the IPTP in the subtropics. When the conveyer belt approaches the TP, part of its water vapor is hauled away and turned northward, then lifted upward by the IPTP-SHAP, resulting in heavy precipitation in the monsoon trough over northern India and along the foothills and slopes of the TP. The rest of the water vapor along the water conveyer belt is transported northeastward to sustain the EASM, which is controlled by the land–sea thermal contrast and thermal forcing of the TP. These results highlight the dominant roles of the land–sea thermal contrast and IPTP thermal forcing in influencing the ASM.

Discussion

In nature, the influences of the IPTP orography and its surface sensible heating cannot be separated. The significance of the dominance of IPTP thermal forcing in influencing the ASM lies in the fact that, over the modern-day orography, the thermal status of the IPTP varies due to natural and anthropogenic factors, as reviewed above. By focusing on changes in the thermal status of the IPTP, the dominance of thermal controls on the ASM may provide us with a tangible way of identifying climate trends in the Asian summer monsoon in a warming world, and of improving weather forecasts, climate predictions, and projections in areas affected by the Asian monsoon.

Methods

General Circulation Model Description. The atmospheric general circulation model (GCM) employed in the present study is SAMIL (Spectral Atmospheric Model of IAP/LASG), as developed at the State Key Laboratory of Numerical Modeling for Atmospheric Sciences and Geophysical Fluid Dynamics/Institute of Atmospheric Physics (LASG/IAP), Beijing, China. SAMIL is a spectral model with rhomboidal truncation at wave-number 42. It has 26 vertical layers with a top at 2.1941 hPa[39]. As

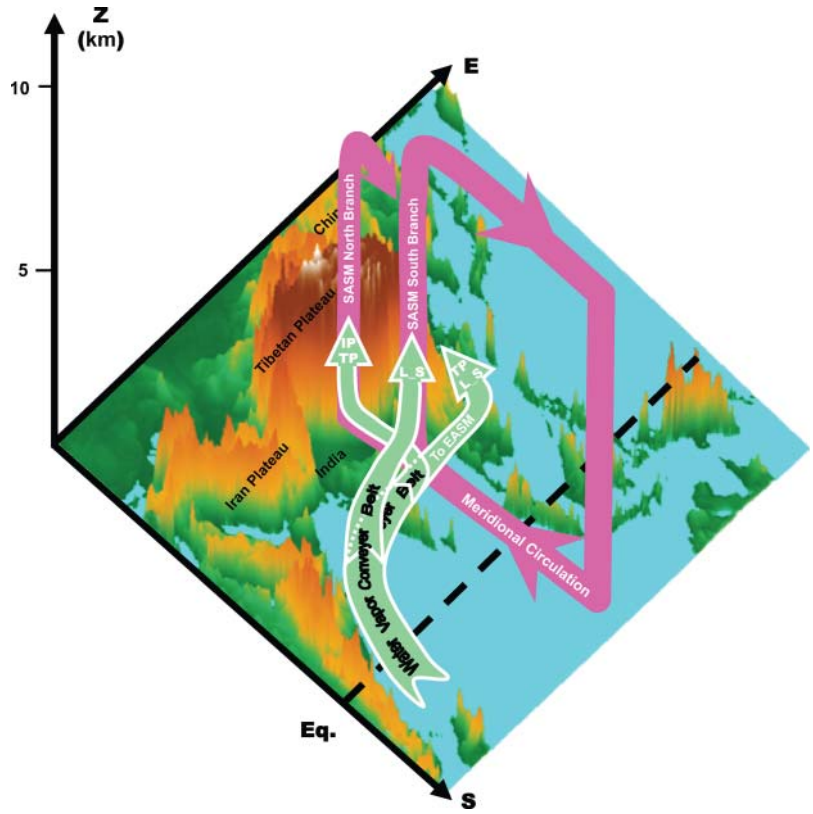

Figure 6 | Schematic diagram showing the gross structure of the South Asian summer monsoon. For the southern branch, water vapor along the conveyer belt is lifted up due mainly to land–sea (L_S) thermal contrast in the tropics; for the northern branch the water vapor is drawn away from the conveyer belt northward toward the foothills and slopes of the TP, and is uplifted to produce heavy precipitation that is controlled mainly by IPTP-SHAP; the rest of the water vapor is transported northeastward to sustain the East Asian summer monsoon, which is controlled by the land–sea thermal contrast as well as thermal forcing of the TP.

an atmospheric component of the climate system model FGOALS-s developed at LASG/IAP, SAMIL is driven by the sixth generation of NCAR Coupler using NCAR CLM3 as a land surface component[40]. Its physical parameterizations include SES2[41], the updated radiation parametric scheme developed by Edwards and Slingo[42], diagnostic cloud parameterization, the mass flux cumulus parameterization of Tiedtke[43] for deep, shallow, and mid-level convection, and a nonlocal PBL parameterization scheme[44]. Observed mean monthly sea surface temperature (SST) and sea ice with a seasonal cycle, as obtained from AMIP II[45], were prescribed. All experiments were integrated for 7 years, and the monsoon climate was calculated from the last five June–August periods.

Experiment Design. The model was integrated with prescribed, seasonally varying SST and sea ice to form a controlled- climate integration first, which is referred to as the **CON** experiment.

The orographic setting in each experiment was achieved by changing only the prescribed surface elevations. The no-surface-sensible-heating experiments were designed as follows: while the surface energy balance was kept unchanged, the surface sensible heat released at the elevation above 500 m was not allowed to heat the atmosphere; i.e., the vertical diffusive heating term in the atmospheric thermodynamic equation was set to zero. Details of the design for each experiment are given in Table 1 and explained below.

- Influence of Land–Sea Thermal Contrast on the ASM
  For experiments **NMT** and **L_S** (see Fig. 1): the elevation over the whole globe is set to zero in **NMT**. Since the main purpose of this study is to compare the relative contributions of land–sea thermal contrast and large-scale Asian mountain ranges on different parts of the ASM, in the **L_S** experiment only the elevations of the Iranian Plateau and Tibetan Plateau are set to zero.

- Influence of IPTP Mechanical Insulation on ASM
  For the mechanical forcing experiments **IPTP_M**, **IP_M**, and **TP_M** (see Fig. 2), the Iranian Plateau and Tibetan Plateau together, the Iranian Plateau alone, and the Tibetan Plateau alone are retained from the **CON** experiment, respectively, but their surface sensible heating is not allowed to warm the atmosphere.

- Influence of IPTP Thermal Forcing on the ASM
  In designing the thermal forcing experiments **IP_SH**, **TP_SH**, and **IPTP_SH** (see Fig. 3), three no-surface-sensible-heating experiments (**IP_NS**, **TP_NS**, and **IPTP_NS**) were first designed and integrated, in which the global orographic distribution is the same as in the **CON** experiment while the surface sensible heating on the atmosphere over the IP, TP, and IPTP, respectively, was removed from the **CON** experiment. Because the only difference between the **CON** and **IP-NS (TP_NS, IPTP_NS)** experiments is whether the elevated surface sensible heating on the atmosphere occurs over the IP (TP, IPTP), their integration differences in Fig. 3a (Fig. 3b, 3c) are qualitatively considered as the thermal impact of the IP (TP, IPTP) on the ASM, and are assigned as the **IP_SH** (**TP_SH**, **IPTP_SH**) experiment.

In designing the **HIM** and **HIM_NS** experiments (see Fig. 4), we followed exactly the original work of Boos and Kuang[29]. The **HIM** experiment is the same as **CON** except for "removing the bulk of the Tibetan Plateau while preserving a zonal elongated band of mountains to the south, east and west of the plateau," as denoted by the polygon in Fig. 4c and 4d. The **HIM_NS** experiment is the same as the **HIM**, except that the surface sensible heat flux on the **HIM** mountain surfaces is not allowed to heat the atmosphere.

1. Webster, P. J. *et al.* Monsoons: Processes, Predictability and the prospects for prediction. *J. Geophys. Res.* **103**, 14451–14510 (1998).
2. Meehl, G. A. Coupled ocean-atmosphere-land processes and South Asian monsoon variability. *Science* **265**, 263–267 (1994).
3. Flohn, H. Large-scale aspects of the "summer monsoon" in South and East Asia. *J. Meteor. Soc. Japan* **75th Ann. Vol.** 180–186 (1957).
4. Chang, C. P. *et al. East Asian monsoon* (World Scientific, New Jersey, 2004).
5. Wang, B. *et al. The Asian Monsoon* (Springer, Chichester, 2006).
6. Yeh, T. C., Lo, S.-W. & Chu, P.-C. The wind structure and heat balance in the lower troposphere over Tibetan Plateau and its surrounding. *Acta Meteor. Sinica* **28**, 108–121 (1957).
7. Ye, D. Z., & Gao, Y. X. *Meteorology of the Qinghai-Xizang Plateau* (Chinese Science Press, Beijing, 1979).
8. Yanai, M., Li, C. F., & Song, Z. S. Seasonal heating of the Tibetan Plateau and its effects on the evolution of the Asian Summer Monsoon. *J. Meteor. Soc. Japan* **70**, 319–351 (1992).
9. Yanai, M. & Wu, G.-X. Effects of the Tibetan Plateau *Chapter 13, The Asian Monsoon* (eds Wang, B. *et al*) (Springer, Chichester, 2006).
10. Chang, C.-P., Wang, Z., Hendon, H. 2006: The Asian winter monsoon. *Chapter 3, The Asian Monsoon* (eds Wang, B. *et al.*) (Springer, Chichester, 2006).

11. Wu, G. X. *et al*. Sensible heat driven air-pump over the Tibetan Plateau and its impacts on the Asian Summer Monsoon, Collections on the Memory of Zhao Jiuzhang (eds Ye, D. Z. *et al*) (Chinese Science Press, Beijing, 1997).
12. Wu, G. X. *et al*. The Influence of the Mechanical and Thermal Forcing of the Tibetan Plateau on the Asian Climate. *J. Hydrometeorology.* **8**, 770–789 (2007).
13. Held, I. M. Stationary and quasi-stationary eddies in the extra-tropical troposphere: Theory. *Large-Scale Dynamical Processes in the Atmosphere* (eds Hoskins, B. J. & Pearce, R. P.) (Academic Press, London, 1983).
14. Chen, P. Thermally Forced Stationary Waves in a Quasigeostrophic System. *J. Atmos. Sci.* **58**, 1585–1594 (2001).
15. Lau, N. C. & Wang, B. Interactions between the Asian monsoon and the El Niño/ Southern oscillation. *Chapter 12, The Asian Monsoon* (eds Wang, B. *et al*.) (Springer, Chichester, 2006).
16. Li, T. Monsoon climate variabilities. *Climate Dynamics: Why Does Climate Vary?*"(eds Sun, D.-Z. & Frank, B. doi:10.1029/2008GM000782.) (Geophys. Monogr. Ser., 2010)
17. Wu, G. X., Liu, Y., Zhu, X., Li, W., Ren, R., Duan, A. & Liang, X. Multi-scale forcing and the formation of subtropical desert and monsoon. *Ann. Geophys.* **27**, 3631–3644 (2009)
18. Allan, R. P. Human influence on rainfall. *Nature*, **470**, 17 February, 345 (2011).
19. Ramanathan, V. & Carmichael, G. Global and regional climate changes due to black carbon. *Nature geoscience* doi:10.1038/ngeo156, Published online: 23 March 2008. 221–227 (2008).
20. Duan, A. M., Wu, G. X., Zhang, Q. & Liu, Y. M. New Proofs of the recent climate warming over the Tibetan Plateau as a result of the increasing greenhouse gases emissions. *Chinese Sci. Bulletin* **51** (11), 1396–1400 (2006).
21. Duan, A. M. & Wu, G. X. Weakening Trend in the Atmospheric Heat Source over the Tibetan Plateau during Recent Decades. Part I: Observations. *J. Climate.* **21**, 3149–3164 (2008).
22. Ramanathan, V. *et al*. Atmospheric brown clouds: impacts on South Asian climate and hydrologic cycle. *Proc. Natl Acad. Sci. USA* **102**, 5326–5333 (2005).
23. Chung, C. & Ramanathan, V. Relationship between trends in land precipitation and tropical SST gradient. *Geophys. Res. Lett.* **34**, doi10.1029/2007GL030491 (2007).
24. Clarke, A. & Noone, K. Soot in the Arctic: a cause for perturbation in radiative transfer. *J. Geophys. Res.* **19**, 2045–2053 (1985).
25. Warren, S. & Wiscombe, W. Dirty snow after nuclear war. *Nature* **313**, 467–470 (1985).
26. Lau, W. K. M., Kim, M.–K., Kim, K. M. & Lee, W. S. Enhanced surface warming and accelerated snow melt in the Himalayas and Tibetan Plateau induced by absorbing aerosols. *Environ. Res. Lett.* **5**, 025204 (2010).
27. Ramana, M. V., Ramanathan, V., Podgorny, I. A., Pradhan, B. & Shrestha, B. The direct observations of large aerosol radiative forcing in the Himalayan region. *Geophys. Res. Lett.* 31 L05111 (2004).
28. Solomon, S. *et al. Contribution of Working Group I to the Fourth Assessment Report of the Intergovernmental Panel on Climate Change* (Cambridge Univ. Press, London, 2007).
29. Boos, W. R. & Kuang, Z. M. Dominant control of the South Asian monsoon by orographic insulation versus plateau heating. *Nature* **463**, 218–223 (2010).
30. Adler, R. F. *et al*. The Version 2 Global Precipitation Climatology Project (GPCP) Monthly Precipitation Analysis (1979-present). *J. Hydrometeor.* **4** ,1147 (2003).
31. Kanamitsu, M. *et al*. 2002: NCEP-DEO AMIP-II Reanalysis (R-2). *Bull. Amer. Meteor. Soc.* **83**, 1631–1643.
32. Emanuel, K. A., Neelin, J. D. & Bretherton, C. S. On large-scale circulations in convecting atmospheres. *Q. J. R. Meteor. Soc.* **120**, 1111–1143 (1994).
33. Holton, J. R. *An introduction to dynamic meteorology* (Elsevier Academic Press, Amsterdam, 2004).
34. Queney, P. The problem of air flow over mountain: a summary of the theoretical studies. *Bull. Amer. Meteor. Soc.* **29**, 16–26 (1948).
35. Wu, G. X. Recent Progress in the Study of the Qinghai-Xizhang Plateau Climate Dynamics in China. *Quarternary Sci.* **24**, 1–9 (2004)
36. Wu, G. X. The nonlinear response of the atmosphere to large-scale mechanical and thermal forcing. *J. Atmos. Sci.* **41**, 2456–2476 (1984).
37. Yanai, M. & Li, C. Mechanism of heating and the boundary layer over the Tibetan Plateau. *Mon. Wea. Rev.* **122**, 305–323 (1994).
38. Eady, E. T. The cause of the general circulation of the atmosphere. *Centen. Proc. Roy. Meteor. Soc.* 156–172 (1950)
39. Wu, T. W. *et al*. The performance of atmospheric component model R42L9 of GOALS/LASG. *Adv. Atmos. Sci.* **20**, 726–742 (2003).
40. Bao, Q. *et al*. An introduction to the coupled model FGOALS1.1-s and its performance in East Asia. *Adv. Atmos. Sci.* **27**, 1131–1142 (2010).
41. Sun, Z. Parameterizations of radiation and cloud optical properties. *BMRC Research Report*. 107–112 (2005).
42. Edwards, J. M. & Slingo, A. Studies with a flexible new radiation code. I: Choosing a configuration for a large-scale model. *Q.J. Roy. Meteorol. Soc.* **122**, 689–720 (1996).
43. Tiedtke, M. A. comprehensive mass flux scheme for cumulus parameterization in large-scale models. *Mon. Wea. Rev.* **117**, 1779–1800 (1989).
44. Holtslag, A. A. M. & Boville, B. A. Local versus nonlocal boundary-layer diffusion in a global climate model. *J. Climate.* **6**, 1825–1842 (1993).
45. TaylorK, E., Williamson, D. & Zwiers, F. The sea surface temperature and sea-ice concentration boundary conditions for AMIP II simulations. PCMDI Report No. 60, 25 pp, (2000).

Acknowledgments

This study was jointly supported by the MOST Programme No. 2010CB950400, 2012CB417200, and the NSFC Projects Nos. 40875034 and 40925015. FFJ was supported by NSF ATM 1034439, NOAA NA10OAR4310200, and DOE DESC0005110.

Author contributions

All authors contributed to designing the research and interpreting results. Q. B. and B.H. performed the model runs, and G.X.W. and B.H. plotted the figures. G.X.W., Y.M.L., A.M.D., and F.F.J. prepared the main text.

Additional information

Competing financial interests: The authors declare no competing financial interests.

How to cite this article: Wu, G. *et al*. Thermal Controls on the Asian Summer Monsoon. *Sci. Rep.* **2**, 404; DOI:10.1038/srep00404 (2012).